rIgG1 Fc Hexamer Inhibits Antibody-Mediated Autoimmune Disease via Effects on Complement and FcγRs

Rolf Spirig,*[,1] Ian K. Campbell,[†,1] Sandra Koernig,[†] Chao-Guang Chen,[†] Bonnie J. B. Lewis,[‡,§] Rebecca Butcher,[†] Ineke Muir,[†] Shirley Taylor,[†] Jenny Chia,[†] David Leong,[†] Jason Simmonds,[†] Pierre Scotney,[†] Peter Schmidt,[†] Louis Fabri,[†] Andreas Hofmann,* Monika Jordi,* Martin O. Spycher,* Susann Cattepoel,* Jennifer Brasseit,* Con Panousis,[†] Tony Rowe,[†] Donald R. Branch,[‡,§] Adriana Baz Morelli,[†] Fabian Käsermann,* and Adrian W. Zuercher*

Activation of Fc receptors and complement by immune complexes is a common important pathogenic trigger in many autoimmune diseases and so blockade of these innate immune pathways may be an attractive target for treatment of immune complex-mediated pathomechanisms. High-dose IVIG is used to treat autoimmune and inflammatory diseases, and several studies demonstrate that the therapeutic effects of IVIG can be recapitulated with the Fc portion. Further, recent data indicate that recombinant multimerized Fc molecules exhibit potent anti-inflammatory properties. In this study, we investigated the biochemical and biological properties of an rFc hexamer (termed Fc-μTP-L309C) generated by fusion of the IgM μ-tailpiece to the C terminus of human IgG1 Fc. Fc-μTP-L309C bound FcγRs with high avidity and inhibited FcγR-mediated effector functions (Ab-dependent cell-mediated cytotoxicity, phagocytosis, respiratory burst) in vitro. In addition, Fc-μTP-L309C prevented full activation of the classical complement pathway by blocking C2 cleavage, avoiding generation of inflammatory downstream products (C5a or sC5b-9). In vivo, Fc-μTP-L309C suppressed inflammatory arthritis in mice when given therapeutically at approximately a 10-fold lower dose than IVIG, which was associated with reduced inflammatory cytokine production and complement activation. Likewise, administration of Fc-μTP-L309C restored platelet counts in a mouse model of immune thrombocytopenia. Our data demonstrate a potent anti-inflammatory effect of Fc-μTP-L309C in vitro and in vivo, likely mediated by blockade of FcγRs and its unique inhibition of complement activation. ***The Journal of Immunology*****, 2018, 200: 2542–2553.**

Antibody-mediated autoimmune diseases can give rise to immune complexes that are not readily cleared from the circulation but instead become highly pathogenic by engaging Fc receptors, activating complement, and initiating inflammatory pathways (1, 2). Ideally, an effective therapeutic would target these key innate immune pathways.

Plasma-derived IgG that is administered either i.v. (as IVIG) or s.c. has been increasingly used at high dose for the treatment of patients with chronic or acute autoimmune and inflammatory diseases, such as immune thrombocytopenia (ITP), Guillain-Barré syndrome, Kawasaki disease, chronic inflammatory demyelinating polyneuropathy, myasthenia gravis, and several other rare diseases (3). In addition, IVIG is currently under evaluation for many other diseases such as rheumatoid arthritis (4).

Several mechanisms of action have been proposed for the anti-inflammatory effect of high-dose IVIG (5, 6). Some of these are dependent on the $F(ab')_2$ portion and include neutralization of autoantibodies by anti-idiotypic Abs (7, 8) and binding/neutralization of immune mediators, such as cytokines (9). Other protective mechanisms are mediated by the Fc domain and include blockade of FcγRs (10), saturation of the neonatal Fc receptor (FcRn) to enhance autoantibody clearance (11), scavenging of complement protein fragments (12) or modulation of immune cell activity (regulatory T cells, B cells, or tolerogenic

*CSL Behring AG, 3010 Bern, Switzerland; [†]CSL Ltd., Bio21 Institute, Parkville, Victoria 3010, Australia; [‡]Centre for Innovation Canadian Blood Services, Toronto, Ontario K1G 4J5, Canada; and [§]Department of Medicine, University of Toronto, Toronto, Ontario M5G 2M1, Canada

[1]R.S. and I.K.C. contributed equally to this work.

ORCIDs: 0000-0002-3731-966X (I.K.C.); 0000-0003-2136-8595 (C.-G.C.); 0000-0002-8209-1385 (I.M.); 0000-0002-3718-4363 (S.T.); 0000-0003-1947-8701 (J.S.); 0000-0002-8974-2451 (D.R.B.); 0000-0002-4255-9350 (F.K.).

Received for publication August 15, 2017. Accepted for publication February 13, 2018.

This work was supported by a Canadian Blood Services Graduate Fellowship Program award (to B.J.B.L.), CSL Ltd./CSL Behring (to D.R.B.), and the Canadian Blood Services Centre for Innovation (to D.R.B.).

R.S. and I.K.C. designed, performed, analyzed, and interpreted experiments and wrote the manuscript. S.K. and C.-G.C. designed, performed, analyzed, and interpreted experiments and revised the manuscript. B.J.B.L., R.B., I.M., S.T., J.C., D.L., J.S., P. Scotney, P. Schmidt, L.F., A.H., M.J., M.O.S., S.C., and J.B. performed, analyzed, and interpreted experiments and revised the manuscript. C.P., T.R., and D.R.B. designed and interpreted experiments, and revised the manuscript. A.B.M., F.K., and A.W.Z. designed and interpreted experiments, and wrote the manuscript.

Address correspondence and reprint requests to Dr. Adrian W. Zuercher and Dr. Rolf Spirig, CSL Behring AG, Research, Wankdorfstrasse 10, 3010 Bern, Switzerland. E-mail addresses: adrian.zuercher@cslbehring.com (A.W.Z.) and rolf.spirig@cslbehring.com (R.S.)

The online version of this article contains supplemental material.

Abbreviations used in this article: ADCC, Ab-dependent cell-mediated cytotoxicity; A4F, asymmetric flow field–flow fractionation; AP, alternative pathway; CAbIA, collagen Ab–induced arthritis; CIA, collagen-induced arthritis; CII, type II collagen; CP, classical pathway; FcRn, neonatal Fc receptor; HAGG, heat-aggregated γ globulin; IRB-SRC, Interregional Blood Transfusion Service SRC; ITP, immune thrombocytopenia; LP, lectin pathway; MALS, multiangle light scattering; NHS, normal human serum; SEC, size exclusion chromatography; Tg, transgenic; WT, wild-type.

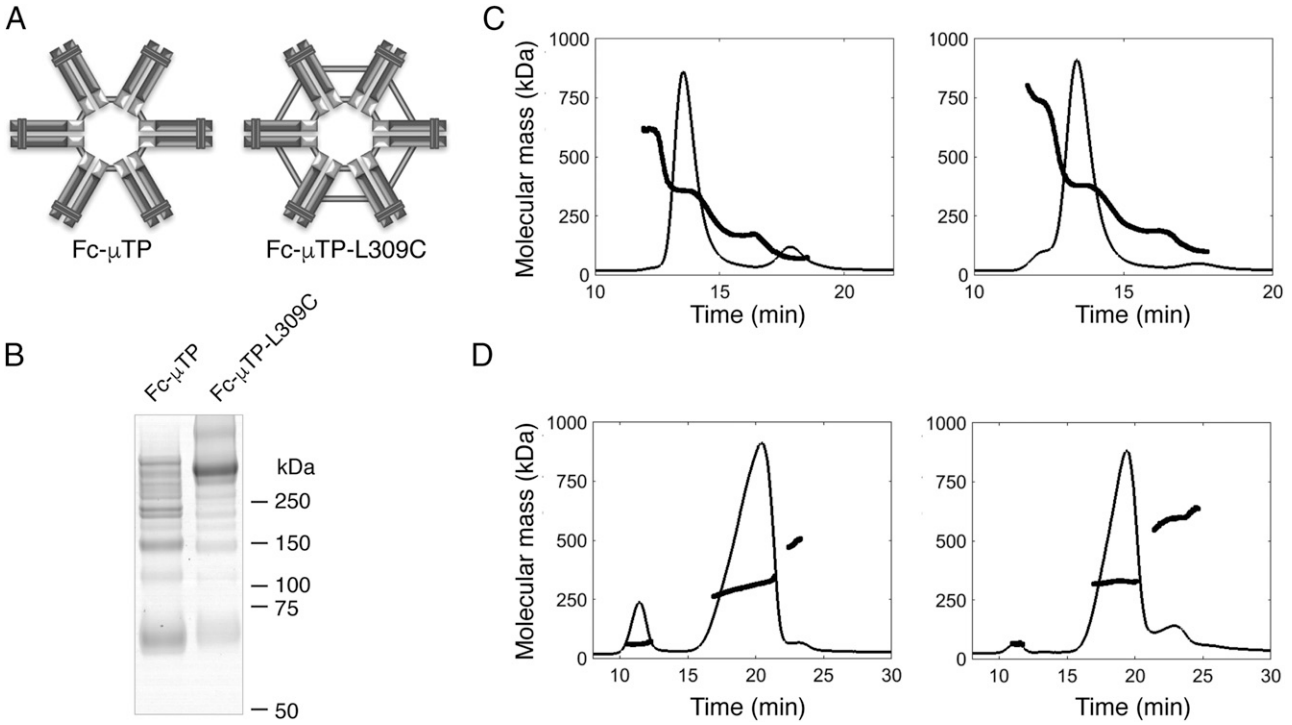

FIGURE 1. Biochemical characterization of rFc multimers. (**A**) Schematic diagram of Fc-μTP and Fc-μTP-L309C hexamer structures. Light gray bars represent presumed disulphide bonds. (**B**) SDS-PAGE of Fc-μTP (left) and Fc-μTP-L309C (right) rFc multimers. Molecular mass markers in kDa are shown. (**C**) SEC and (**D**) A4F with MALS of Fc-μTP (left panels) and Fc-μTP-L309C (right panels). Chromatograms show the normalized UV (280 nm) signals, and the bold lines are the molecular mass (in kDa) of material eluted at the time indicated.

DCs), for example, by upregulation of inhibitory FcγRIIb (CD32b) (13). A therapeutic role for the IgG Fc domain in autoimmune diseases has been suggested in experimental models of arthritis and ITP (13, 14). Furthermore, in a clinical study, plasma-derived monomeric Fc successfully alleviated acute ITP in children (15).

Recent studies have investigated the in vivo efficacy of rFc protein-based therapeutics. In particular, various approaches for controlled multimerization of Fc to form polyvalent molecules have been explored (16). Fusion of the human IgG2 hinge region to human IgG1 Fc or mouse IgG2a Fc led to expression of multimerized Fc fragments that bound FcγR with high avidity (17). These molecules demonstrated therapeutic efficacy in animal models of arthritis and ITP (17), as well as in a model of inflammatory neuropathy (18) and in experimental autoimmune myasthenia gravis (19). Interestingly, in most models, efficacy was achieved with low doses of ~50 mg/kg body weight, compared with the standard dose of 1000–2000 mg/kg for IVIG in inflammatory indications. Using an alternative strategy, Ortiz et al. (20) studied Fc multimers of increasing valency and identified molecules that bound FcγRs with high avidity without triggering activating signals. A trivalent molecule termed Fc3Y showed protection in mouse models of ITP, arthritis, and epidermolysis bullosa acquisita (20). Finally, a hexameric Fc molecule showed increased binding to FcγRs and dendritic cell–specific intercellular adhesion molecule-3 grabbing nonintegrin, appeared to fully activate complement (C1q binding and C5b-9 deposition) (21), and effectively interfered with FcγR function (22). Ab hexamer structures are reported to have superior complement fixing properties; indeed, upon binding to cell-surface Ags, IgG monomers spontaneously arranged into ordered hexamer structures that recruited and activated C1 (23). None of the molecules described earlier have progressed into human trials, and their protective mechanisms of action have not been fully elucidated.

We developed a hexameric rFc multimer and compared its therapeutic efficacy and mechanism of action with that of IVIG and rFc monomer in autoantibody-driven disease models. The multimer demonstrated high-avidity binding to FcγRs and inhibition of FcγR-mediated effector functions; furthermore, it was unique among this class of molecules in also inhibiting the full activation of complement. A rapid and pronounced therapeutic efficacy was observed in mouse models of inflammatory arthritis and ITP.

Materials and Methods

Generation of Fc-μTP and Fc-μTP-L309C expression constructs

Fc-μTP was generated by fusing the 18-aa residues (PTLYNVSLVMSDTAGTCY) of human IgM μ-tailpiece to the C terminus of the C region of human IgG1 Fc fragment (aa residues 216–447, EU numbering; UniProtKB P01857). Fc-μTP-L309C was generated by mutating the Leu residue at 309 (EU numbering) of Fc-μTP to Cys.

The DNA fragments encoding Fc-μTP and Fc-μTP-L309C were synthesized and codon optimized for human cell expression by Thermo Fisher Scientific (Waltham, MA). The DNA fragments were cloned between ApaLI and XbaI sites of pRhG4 mammalian expression vector with an InTag adaptor for positive selection as described previously (24). Miniprep plasmid DNA was purified using the QIAprep Spin Miniprep kit (Qiagen, Hilden, Germany), and the sequence was confirmed by DNA sequencing analysis. Restriction enzymes and T4 DNA ligases were purchased from New England BioLabs (Ipswich, MA).

Transient expression in Expi293 cells

Fc-μTP and Fc-μTP-L309C, as well as fragments of human FcγRs CD16a, CD32a, CD32b/c and CD64, were produced by transient transfection using the Expi293 Expression System (Thermo Fisher Scientific) according to the manufacturer's instruction and as described recently (25, 26). rFc preparations were purified using standard Protein A affinity purification techniques. The recombinant products used in this study (Fc, Fc-μTP, and Fc-μTP-L309C) were shown to be endotoxin-free by the limulus amebocyte lysate test and based on their inability to stimulate NF-κB activation in THP1 cells (data not shown).

Table I. Biochemical characterization of rFc multimers

rFc Molecule[a]	Technique	Monomer (%)	Dimer (%)	Trimer (%)	Hexamer (%)	Multimer (%)
Fc-μTP	SEC-MALS	13 (73 kDa)		2 (168 kDa)	84 (355 kDa)	
	A4F-MALS	10 (60 kDa)			87 (305 kDa)	3 (491 kDa)
Fc-μTP-L309C	SEC-MALS		4 (114 kDa)	4 (211 kDa)	84 (383 kDa)	8 (745 kDa)
	A4F-MALS	2 (62 kDa)			83 (327 kDa)	15 (592 kDa)

[a]rFc multimers were analyzed as described in Fig. 1C and 1D. Data show the percentage of material that was identified as monomer, dimer, trimer, hexamer, and multimer (dodecamer). The corresponding molecular masses (in kDa) are indicated in brackets.

Size exclusion chromatography–multiangle light scattering

Size exclusion chromatography–multiangle light scattering (SEC-MALS) was performed using an Agilent 1200 series HPLC in series with a Wyatt DAWN Heleos II EOS MALS detector and Wyatt Optilab T-rEx refractive index detector. For analysis, 24 μg of Fc-μTP-L309C was injected onto a 4.6 × 300 mm WTC-030N5 SEC column (Wyatt Technology, Santa Barbara, CA) at room temperature. Isocratic elution was performed with PBS as mobile phase and a flow rate of 0.2 ml/min. Data were analyzed with Astra 6 software (Wyatt Technology) using a refractive index increment value of 0.185 ml/g.

Asymmetrical flow field-flow fractionation-MALS

Samples were tested using a Postnova AF2000 asymmetrical flow field–flow fractionation (A4F) coupled with Wyatt HELEOS light scattering and Optilab rEX refractive index detectors and a Shimadzu PDA detector. The concentration and size data were collected with Wyatt's Astra 5 software and analyzed using Astra 6.1. The A4F channel was equipped with a regenerated cellulose membrane with a molecular mass cutoff of 10 kDa and a 350-μm spacer.

Binding to FcγRs and FcRn by Biacore and Octet analyses

Binding to FcγRs was carried out using a Biacore T200 biosensor (GE Healthcare, Waukesha, WI). Recombinantly expressed FcγR components CD16a, CD32a, CD32b/c, and CD64 were captured via their His tags on a nitrilotriacetic acid sensor chip, precharged with Ni^{2+}, and the surface washed with 3 mM EDTA. Fc-μTP-L309C was injected over captured receptors for 3 min at 100 nM, and dissociation was monitored for a further 30 min. After each injection, the surface was regenerated with a 60-s injection of 350 mM EDTA and 30-s injection of 50 mM NaOH. Sensorgrams were double

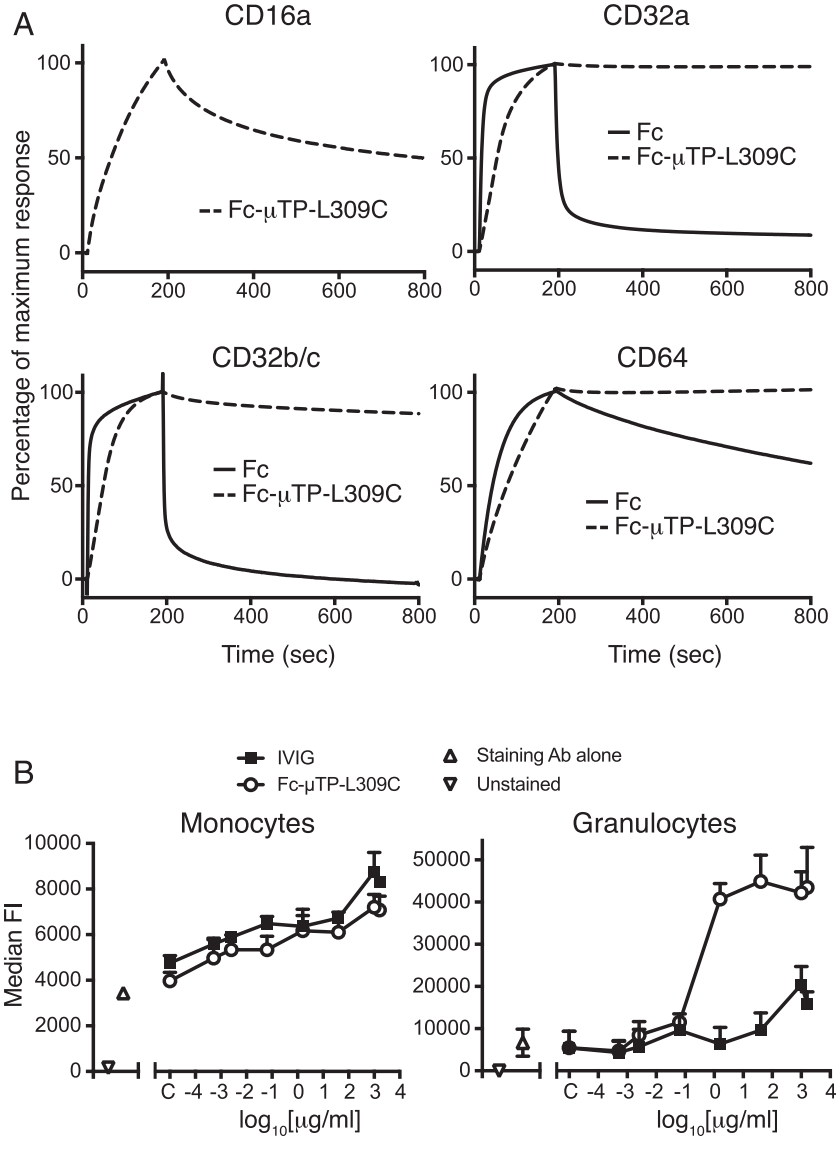

FIGURE 2. Binding of Fc-μTP-L309C to Fc receptor. (**A**) Biacore analysis of binding of Fc-μTP-L309C to FcγR components CD16a, CD32a, CD32b/c, and CD64. Affinity of monomeric Fc to CD16 was too low to generate a signal. (**B**) Binding of Fc-μTP-L309C and IVIG to primary human monocytes and granulocytes. Data shown as mean + SEM, $n = 3$ individual experiments using cells from three different donors.

referenced by subtraction of signals from a blank injection, and a reference cell with no protein was captured. Running buffer throughout was 10 mM HEPES, 150 mM NaCl (pH 7.3). The analysis temperature was 37°C using a flow rate of 30 μl/min.

Binding to FcRn at pH 6 (Sino Biological, Peking, China) was analyzed in a 96-well format on an Octet QKe device (FortéBio, Menlo Park, CA). The assays were visualized with the Octet Software 7.0.1.1 (FortéBio).

FACS evaluation of Fc-μTP-L309C binding to human granulocytes and monocytes

Cells were isolated from buffy coats obtained from healthy blood donors (Interregional Blood Transfusion Service SRC [IRB-SRC], Bern, Switzerland) by density gradient centrifugation over Ficoll-Paque (GE Healthcare). Granulocytes were isolated from the lowest layer with additional hypotonic lysis of the remaining erythrocytes. Monocytes were isolated from PBMCs using a CD14 microbeads kit (Miltenyi Biotec, Bergisch Gladbach, Germany). Cells were incubated with Fc-μTP-L309C or IVIG (CSL Behring AG, Bern, Switzerland) for 45 min at 4°C, washed four times with PBS containing 0.1% BSA (Sigma) and 0.01% NaN_3 (Sigma), and stained with a FITC-labeled goat polyclonal $F(ab')_2$ Ab-fragment against human IgG (ab98534; Abcam) for 45 min at 4°C. Stained cells were washed a further four times and then analyzed with a BD FACSCanto II flow cytometer (BD Biosciences AG, Allschwil, Switzerland), and the data were evaluated using FlowJo.

Effect of Fc constructs on fluid-phase complement activation in human serum and whole blood

For the assay, normal human serum (NHS) was diluted 1:5 with GVB^{2+} buffer (Complement Tech) and incubated for 1 h at 37°C. The reaction was stopped by adding EDTA. Activation of human complement in serum was analyzed by the generation of C4a and C5a by ELISA (Quidel, San Diego, CA).

Analysis of complement activation in human whole blood was based on anticoagulation with recombinant hirudin (Sarstedt, Numbrecht, Germany). Whole blood was diluted 1:5 in GVB^{2+} buffer and incubated as described earlier for NHS. Complement activation was analyzed by the generation of C4a and sC5b-9 by ELISA (Quidel).

Binding of Fc constructs to C1q

Binding of rFc constructs to C1q was analyzed by ELISA (Inova Diagnostics, San Diego, CA). Wells were precoated with human C1q, and samples were added to allow binding. After washing of the wells to remove all unbound protein, purified peroxidase-labeled goat anti-human IgG conjugate was added. Unbound protein was removed by a further wash step and bound conjugate visualized with 3,3′,5,5′ tetramethylbenzidine substrate.

Effect of Fc constructs on complement deposition

The effect of Fc constructs on the function of the classical pathway (CP), lectin pathway (LP), and alternative pathway (AP) was examined in the Wieslab Complement System Screen (Euro-Diagnostica, Malmø, Sweden), which is an enzyme immunoassay for the specific detection of the three pathways with deposition of C5b-9 (detected with an anti-$C9^{neoepitope}$ mAb) as a common read-out. Samples were preincubated with 20% NHS diluted with GVB^{2+} buffer as described earlier. After 1-h incubation at 37°C, the samples were transferred to the ELISA plates. Further dilutions were made according to the instructions, that is, 1:101 for the CP and LP and 1:18 for the AP. The complement inhibitor Futhan (FUT-125; nafamostat mesilate; BD Biosciences) was used as a positive control. C1q-depleted serum was purchased from Quidel and purified C1q from Quidel and Complement Tech.

HUVECs were cultured according to the manufacturer's description (Lonza, Visp, Switzerland). For analysis of C3b, C1q, and C4b deposition, HUVECs were opsonized with an anti-CD105 (Endoglin) mAb (MEM-226; ab60902; Abcam) before incubation with 20% NHS diluted in GVB^{2+}(1:5) for 30–60 min at 37°C. C3b deposition was detected using an FITC-conjugated anti-C3c polyclonal Ab (F0201; Dako), anti-C1q polyclonal Ab (F0254; Dako), and anti-C4b polyclonal Ab (F0169; Dako) and quantified by FACS.

Analysis of cleavage of C2 by Western blot

Samples containing equal amounts of human serum (1 μl each) were separated on a 4–12% NuPage Bis-Tris SDS-PAGE gel (Invitrogen) and transferred onto a polyvinylidene difluoride membrane (Invitrogen). Purified plasma-derived C2 was used as an additional control (Complement Tech). Equal loading was controlled by Coomassie staining of an identical gel (GelCode Blue; Thermo Scientific). After blocking the membrane overnight at 4°C with Superblock (Thermo Scientific), we detected C2 using mouse anti-C2 Ab (269716; MAB1936; 1:1000 in Superblock; R&D Systems) with HRP-conjugated goat anti-mouse IgG as the secondary Ab (P0447; 1:1000 in Superblock; Dako). Wash steps were performed with PBS/0.05% Tween 20. Finally, the membrane was developed with a chemiluminescence detection kit (SuperSignal West Pico; Thermo Scientific).

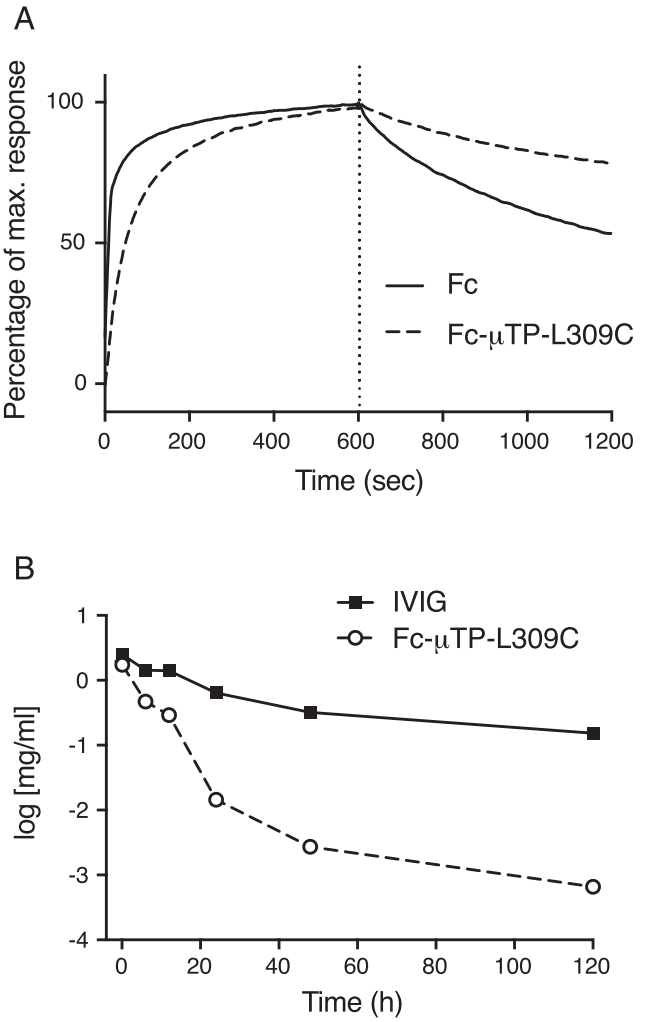

FIGURE 3. Fc-μTP-L309C and the FcRn. (**A**) Binding to FcRn. Octet analysis of binding of Fc and Fc-μTP-L309C (each at 25 μg/ml) to FcRn at pH 6. (**B**) Pharmacokinetics in FcRn-Tg mice. IVIG and Fc-μTP-L309C measured in the blood of FcRn-Tg mice following a single i.v. injection (all doses were 100 mg/kg) at time 0. Data show the means ± range (n = 2); where absent, error bars are smaller than the symbol size.

Respiratory burst in purified human granulocytes and monocytes

Human granulocytes were purified from buffy coats (IRB-SRC Bern) by dextran sedimentation (molecular mass 450–650 kDa) followed by Ficoll gradient centrifugation and hypotonic lysis of residual erythrocytes. A total of 50 μl of granulocytes (2×10^7/ml in HBSS containing 10 mmol/l HEPES, 1 mmol/l $CaCl_2$, 1 mmol/l $MgCl_2$, 1 mg/ml BSA) was added to the wells of a microtiter plate containing 100 μl of luminol solution (0.01 mmol/l PBS; Sigma), and the test articles were added. Chemiluminescence was recorded at 37°C during 90 min, the area under the signal-to-time curve was calculated, and results were expressed as relative light units. Rabbit RBC (Charles River), previously treated with human IgG (CSL Behring) and therefore decorated with human anti-rabbit IgG, were used as positive control.

For inhibition experiments, granulocytes were preincubated with inhibitors (Fc monomer or Fc-μTP-L309C) for 15 min at 37°C, followed by the luminol solution and IgG-treated rabbit RBCs.

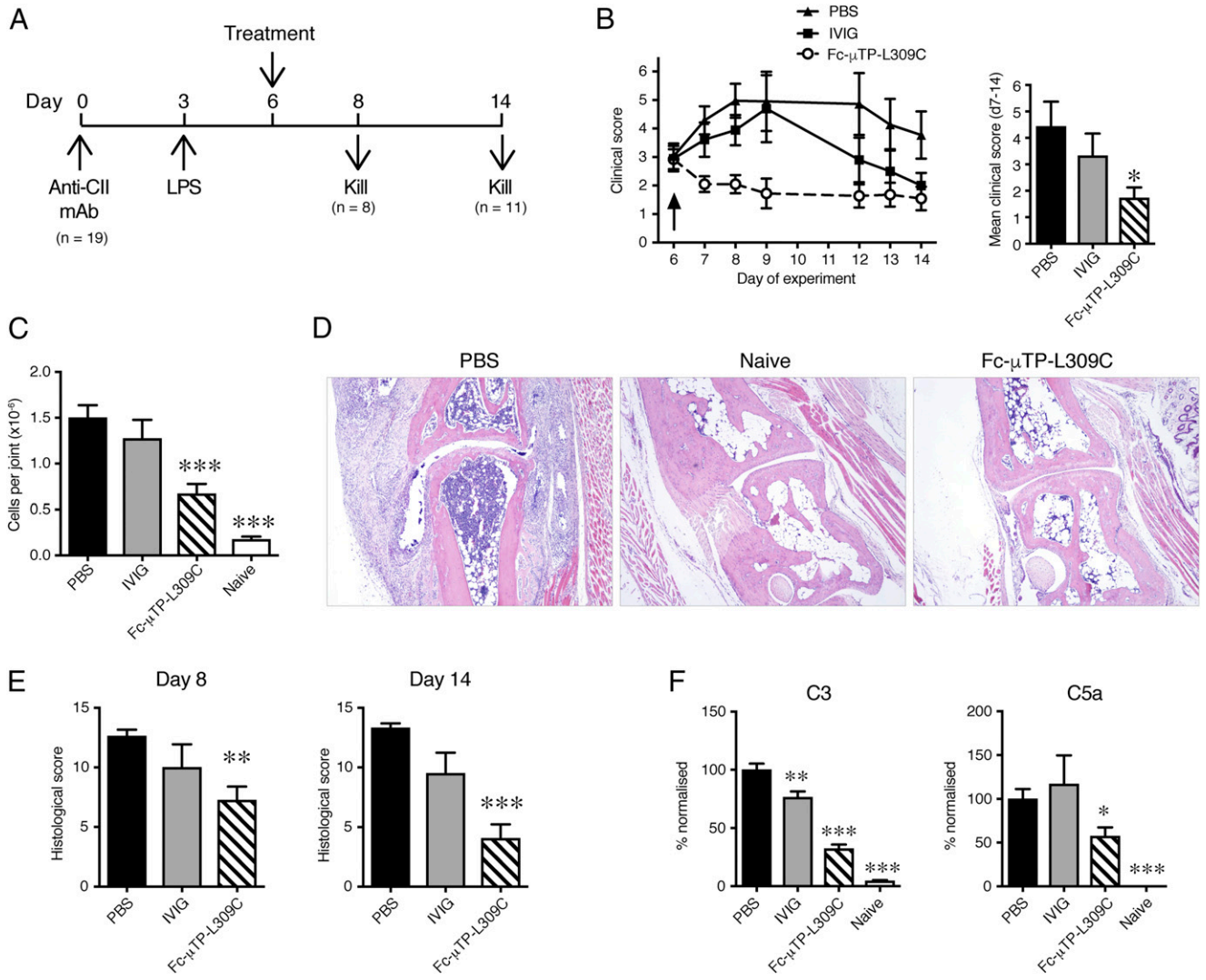

FIGURE 4. Therapeutic effect of Fc-μTP-L309C in acute Ab-mediated arthritis. (**A**) Protocol for evaluating therapeutic efficacy in CAbIA. (**B**) The clinical response to therapeutic administration of Fc-μTP-L309C (200 mg/kg) or IVIG (2000 mg/kg) i.p. at day 6 (arrow). PBS served as control. Kinetics of response (left) and mean clinical scores over days 7–14 (right) are shown. (**C**) $CD45^+$ cells recovered from knee joints of mice at day 8 of disease. (**D**) Histopathology of arthritic joints. Representative H&E-stained sections of tarsal joints from arthritic mice at day 8. The joint of a naive nonarthritic mouse is also shown. Original magnification ×40. (**E**) Histological analysis of joints. Data show the mean (± SEM) histological scores of joints at days 8 and 14. All data are means ± SEM, pooled from two experiments. (**F**) Complement components C3 and C5a in arthritic mouse joint washes taken at day 8, determined by ELISA. Nonarthritic naive mouse joint washes were also included. Data show the complement component concentrations (means ± SEM), which have been normalized as a percentage of the PBS control. $*p < 0.05$, $**p < 0.01$, $***p < 0.001$ compared with PBS control, (B and E) Kruskal–Wallis with Dunn test, (C and F) one-way ANOVA with Dunnett test.

Monocytes were purified from peripheral blood by direct adherence to the wells of the microtiter plates; chemiluminescence was measured as described earlier for granulocytes.

Ab-dependent cell-mediated cytotoxicity assay

PBMCs were isolated from buffy coats obtained from healthy volunteers with blood group O (IRB-SRC Bern) by Ficoll gradient centrifugation. Subsequently, PBMCs were depleted of monocytes by adherence on polystyrene. As target cells, purified human $Rh(D)^+$ RBCs of blood group O volunteers (IRB-SRC Bern) were used. The RBCs were papain treated and labeled with 10 μmol/l CFSE (Molecular Probes) at 1.25×10^6 cells/and then opsonized with anti-D (Rhophylac; CSL Behring).

Lymphocytes (2.2×10^7/ml) were preincubated with inhibitors (IVIG or Fc-μTP-L309C) for 30 min at 37°C; then 100 μl aliquots of the mixtures were added in triplicates to wells of microtiter plates previously incubated with 50 μl of target cells and 50 μl of anti-D (Rhophylac; 6 ng/ml) for 1 h at 37°C. After an overnight incubation at 37°C and 5% CO_2, microtiter plates were centrifuged and washed once with 0.9% NaCl before lysis of the sediment with 1% Triton X-100. Aliquots of the lysates were pipetted into the wells of a microtiter plate and fluorescence was determined (excitation 480 nm/emission 535 nm). Ab-dependent cell-mediated cytotoxicity (ADCC) was calculated using control samples (labeled RBCs without incubation with anti-D) and 100% lysis samples (RBCs treated with Triton X-100).

Phagocytosis assay with THP1 cells

THP1 cells were preincubated with IVIG or Fc-μTP-L309C for 45 min on ice, followed by the incubation with IgG-coated FITC-labeled latex beads (Polysciences, Warrington, PA) for 3 h in the presence of IVIG or Fc-μTP-L309C at 37°C. Afterwards, uptake of beads was analyzed by FACS. As control, Fc receptors were blocked using human Fc receptor binding inhibitor (Fc Block; eBioscience).

Analysis of calcium mobilization in human leukocytes

The effect on Ca^{2+} flux or mobilization of calcium was evaluated in a FACS assay using purified human leukocytes. Cells were incubated with the calcium indicator dye Cal-520 (AAT Bioquest) for 60 min at 37°C, washed, and resuspended in 5 ml of HBSS containing 1 mg/ml BSA/HEPES. Samples were added to FACS tubes, and recording was started. After equilibration, Fc-μTP-L309C or heat-aggregated γ globulin (HAGG;

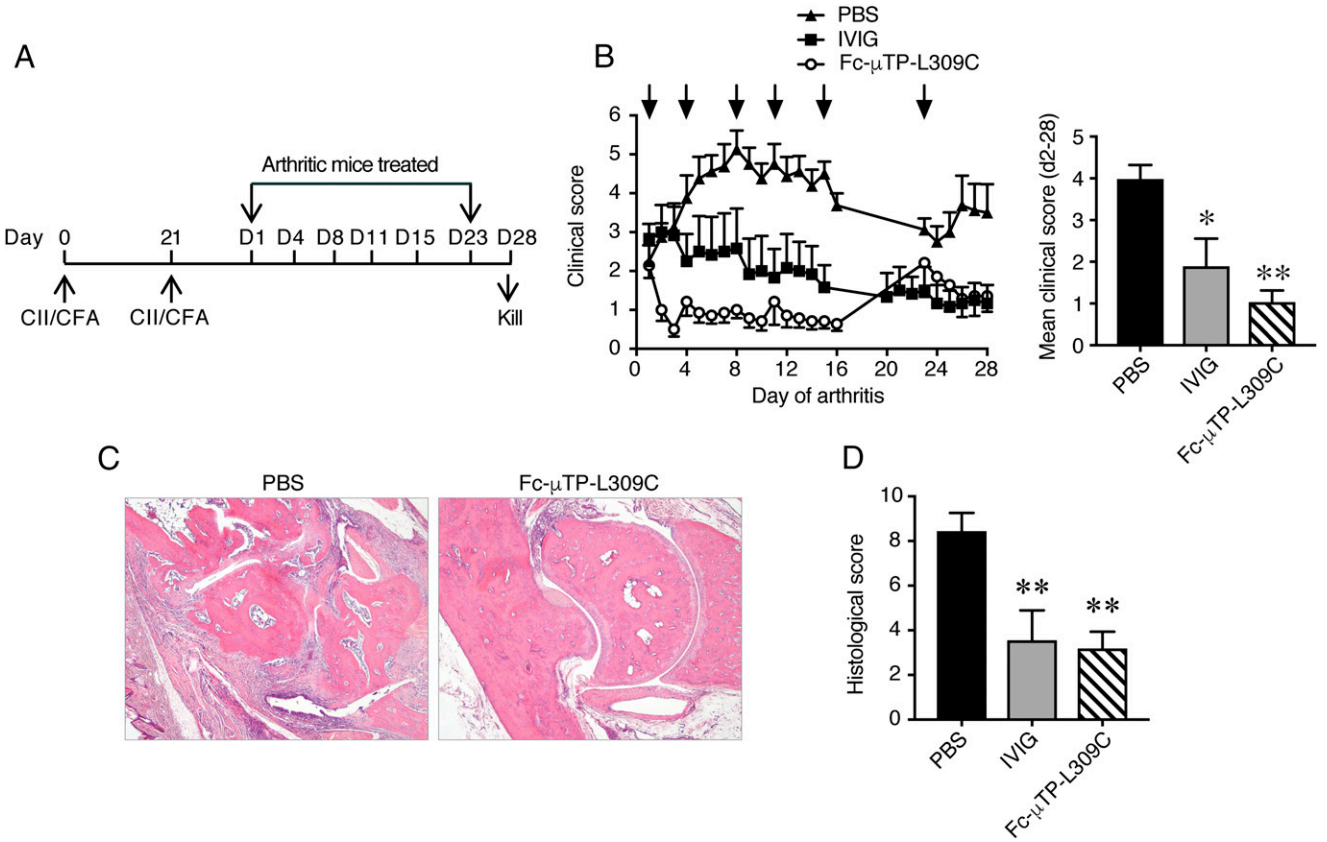

FIGURE 5. Therapeutic effect of Fc-μTP-L309C in chronic autoimmune arthritis. (**A**) Protocol for evaluating therapeutic efficacy in CIA. (**B**) Clinical response to therapeutic administration of Fc-μTP-L309C (200 mg/kg) or IVIG (2000 mg/kg) at the days indicated (arrows). PBS served as control. Kinetics of response (left) and mean clinical scores over days 2–28 (right) are shown (n = 6–8 mice). (**C**) Histopathology of arthritic joints. Representative H&E-stained sections of ankle joints from arthritic mice at day 28 of disease. Joints from IVIG-treated mice (data not shown) appeared similar to the Fc-μTP-L309C group. Original magnification ×40. (**D**) Histological analysis of joints. Data show the mean (± SEM) histological scores of joints (n = 12–16) at day 28 of disease. *$p < 0.05$, **$p < 0.01$ compared with PBS control, Kruskal–Wallis with Dunn test.

control) were added and fluorescence recorded at room temperature for the indicated times. For analysis, cellular subsets were distinguished using forward and side scatter. For inhibition experiments, cells were equilibrated for 1 min before adding rFc multimers; after a 3 min fluorescence recording, activator (HAGG) was added and fluorescence was recorded for another 3 min. Total recording time was 7 min per sample.

Pharmacokinetics of Fc constructs

Human FcRn-transgenic (Tg) mice were injected i.v. or s.c. with IVIG or Fc-μTP-L309C (100 mg/kg). In rats, the doses were 250 mg/kg IVIG and 25 mg/kg Fc-μTP and Fc-μTP-L309C. Serum concentrations were measured with an anti-human IgG1 ELISA (Cayman).

Collagen Ab–induced arthritis

Male BALB/c mice, aged >7 wk, were purchased from the Animal Resources Centre (Canning Vale, WA, Australia) and housed at the University of Melbourne Bio21 Institute animal facility for experimentation. Mouse anti–type II collagen (anti-CII) 5 clone mAb mixture kit was purchased from Chondrex (Redmond, WA). On day 0, mice were injected i.p. with 2 mg of mAb mixture followed by 50 μg of LPS i.p. on day 3. Mice were monitored for up to 14 d for clinical signs of arthritis. A clinical score was assigned by investigators who were blinded to the treatment groups as follows: 0, normal; 0.5, swelling confined to digits; 1, mild paw swelling; 2, marked paw swelling; 3, severe paw swelling and/or ankylosis. Mice that showed signs of arthritis at day 6 (i.e., clinical score ≥1) were given a single i.p. or s.c. injection of rFc multimer, IVIG, or PBS.

Collagen-induced arthritis

Male DBA/1J mice (aged 8–12 wk), obtained from Jackson Laboratories (Bar Harbor, ME) and bred in-house (Bio21 Animal Facility, University of Melbourne), were injected intradermally at the base of the tail with 0.1 ml of emulsion containing equal volumes of chick CII (2 mg/ml in 10 mM acetic acid; Sigma) and CFA (containing 5 mg/ml *Mycobacterium tuberculosis* H37RA; Becton-Dickinson), as described previously (27). The injection was repeated after 3 wk. Mice were assessed daily and recruited on the first day of clinical disease (as detailed earlier) into one of three treatment groups (PBS, 200 mg/kg Fc-μTP-L309C, or 2000 mg/kg IVIG). Mice were given multiple s.c. injections with reagents as detailed in the *Results*.

Histology of arthritic joints

Mice were killed and the left rear paws were fixed in 10% neutral-buffered formalin, decalcified, and embedded in paraffin. Sagittal tissue sections were stained with H&E and scored blinded to the treatment groups. Ankle joints were scored for exudate (presence of inflammatory cells within the joint space), synovitis (degree of synovial membrane thickening and inflammatory cell infiltration), and tissue destruction (cartilage and bone erosion and invasion), each out of 5 (0 = normal, 1 = minimum, 2 = mild, 3 = moderate, 4 = marked, and 5 = severe), and these were tallied for a total score out of 15.

Joint washes and cell digestions

Joint washes and cell digestions were performed as previously described (28). Patellas and surrounding soft tissue (excluding fat) were removed from both rear limbs and placed in RPMI 1640 + 5% FCS on ice for 60 min. The medium was then removed, centrifuged, and the supernatant (joint wash) stored at −30°C until subsequent analysis. The washed patellas and cell pellets were combined for each individual mouse and digested for 30 min at 37°C in a shaking incubator (140 cycles/min) with 1 mg/ml collagenase (CLS-1, 250 U/mg; Worthington Biochemical, Lakewood, NJ) and 0.1 mg/ml DNase I (type IV from bovine pancreas, 2100 kU/mg; Sigma). The digests were strained (70-μm cutoff), washed, and resuspended in PBS + 2% FCS for cell counts and FACS.

FACS analysis of mouse blood and joint digests

Single-cell suspensions of peripheral blood and joint digests were resuspended in PBS containing 2% (v/v) FCS. Cells were stained with the

following anti-mouse mAbs: Ly6C (HK1.4; eBioscience), Ly6G (1A8; BioLegend), CD11b (M1/70; eBioscience), CD16/32 (93; eBioscience), CD64 (X54-5/7.1.1; BD Pharmingen, Mississauga, ON, Canada), and CD45 (30-F11; BD Pharmingen). Fixed cells were acquired on a BD Fortessa and analyzed with FlowJo software.

Protein array of cytokines/chemokines and complement

Joint washes and sera were evaluated for cytokine, chemokine, and complement levels using Luminex-Multiplex (Millipore) and C5a (R&D Systems) and C3 (Geneway) ELISAs.

Murine model of ITP

A passive Ab dose-escalation mouse model of ITP was used (29, 30). In brief, BALB/cJ mice (Jackson Laboratories) were given an i.p. injection of 68 μg/kg anti-platelet mAb (rat anti-mouse glycoprotein IIb; CD41; clone MWReg30; BD Pharmingen) each of 2 d followed by a daily increase in dose of 34 μg/kg platelet Ab for the duration of the experiment. Fc-μTP-L309C or IVIG was given i.p. on day 2 when platelet nadir was attained. Platelet counts were followed daily using FACS (29).

Statistics

Statistical tests were performed using GraphPad Prism 6.0 for Mac OSX or Windows software. Analyses of differences between sample groups were performed using the tests indicated in the text. Data shown are means ± SEM, unless otherwise stated. A p value < 0.05 was considered statistically significant.

Study approval

The CSL/Zoetis Animal Ethics Committees and the University Toronto Health Network Animal Research Committee approved all procedures and protocols.

Results

Development of multimerized Fc molecules by fusing IgG1 Fc with IgM μ-tailpiece

Recombinant human IgG1 Fc was multimerized by fusing the 18-aa IgM μ-tailpiece to the C terminus of either a wild-type (WT) human IgG1 Fc (Fc-μTP) or a variant with a point mutation at position 309 (Fc-μTP-L309C) (31). This resulted in the formation of Fc hexamers, with the point mutation of leucine 309 to cysteine (Fc-μTP-L309C) providing a more stable structure than the WT (Fc-μTP), because of the formation of covalent bonds between Fc molecules (Fig. 1A).

Nonreducing SDS-PAGE of the Protein A–purified rFc multimers showed a laddering pattern for each preparation, corresponding to the expected m.w. for monomer, dimer, trimer, tetramer, pentamer, and hexamers of the Fc fragment. Fc-μTP-L309C, but not Fc-μTP, had a predominant band at the expected m.w. for a hexamer, which is consistent with a more stable structure under the disruptive electrophoresis buffer conditions (Fig. 1B). Higher-order structures, most likely dimers of the hexameric molecule, were also evident for Fc-μTP-L309C.

To examine the multimerization of the Protein A–purified rFc multimers under nondisruptive conditions, we performed SEC and A4F followed by MALS (Fig. 1C, 1D, respectively). Similar distribution patterns with a predominant hexamer peak of ~85% were observed for each of the rFc multimers with both procedures (Table I). The remaining material was mostly lower order (monomer) for Fc-μTP or higher order species (dimers of the hexameric molecule) for Fc-μTP-L309C. Because of its more stable structure, subsequent studies were performed using the Fc-μTP-L309C molecule.

Fc-μTP-L309C binds to FcγRs and primary human myeloid cells

Fc-mediated effects are initiated through the binding of the Fc portion to specific receptors on the surface of leukocytes. To explore whether Fc-μTP-L309C could engage FcγRs, we first examined its qualitative binding to the specific FcγRs, CD16a (FcγRIIIa), CD32a (FcγRIIa), CD32b/c (FcγRIIb/c), and CD64 (FcγRI), by surface plasmon resonance. Fc-μTP-L309C bound to all four receptors and displayed slower apparent off-rates compared with Fc monomer, consistent with an avidity effect either through its binding to multiple immobilized FcγR molecules or rebinding effects (Fig. 2A).

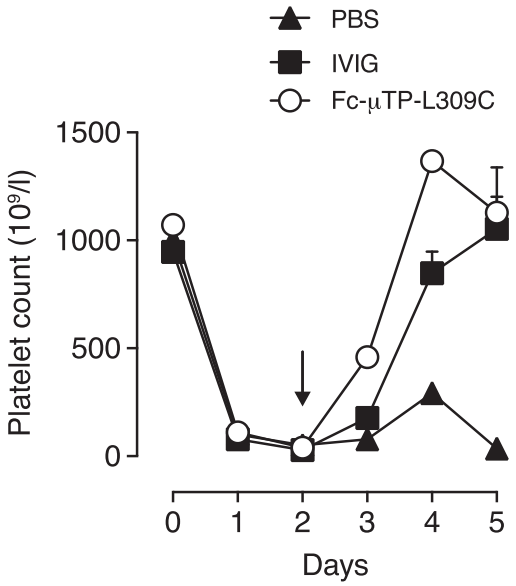

FIGURE 6. Therapeutic effect of rFc multimers in experimental ITP. Dose escalation of anti-platelet Ab (MWReg30) maintains platelet nadir over time. Treatment with a single i.p. dose of Fc-μTP-L309C at day 2 results in alleviation of ITP comparable with IVIG. Shown are the mean platelet values in the blood; data show the mean (± SEM) of platelet counts (Fc-μTP-L309C, $n = 5$; IVIG and PBS, $n = 3$).

Next, the binding of Fc-μTP-L309C to primary human myeloid cells was evaluated by FACS using fluorescently labeled anti-Fc Abs for detection. Fc-μTP-L309C bound to primary human monocytes and granulocytes (Fig. 2B) with higher levels of binding to granulocytes as compared with IVIG.

Fc-μTP-L309C binds to FcRn

The ability of Fc-μTP-L309C to bind FcRn was examined by Octet analysis using immobilized human FcRn at pH 6. Fc-μTP-L309C bound to FcRn with a slower apparent off-rate compared with rFc monomer (Fig. 3A), suggesting an avidity effect.

Pharmacokinetics of Fc-μTP-L309C

The pharmacokinetics of Fc-μTP-L309C was compared with that of IVIG after a single i.v. injection into human FcRn-Tg mice (Fig. 3B). Despite the ability to bind to FcRn with higher avidity (Fig. 3A), Fc-μTP-L309C displayed a more rapid clearance from serum than IVIG, reflected in a shorter serum $t_{1/2}$ (3.1 h). Similar results were obtained in rats ($t_{1/2}$ of 2.5–3.0 h; data not shown).

Fc-μTP-L309C provides therapeutic benefit in acute inflammatory Ab-induced arthritis

Fc-μTP-L309C was examined for therapeutic efficacy in the collagen Ab–induced arthritis (CAbIA) model in mice (14, 28). Disease development in the CAbIA model is dependent on both FcγR engagement and activation of the complement system (32, 33) triggered particularly by the CP (34). Disease was induced in WT BALB/c mice by i.p. injection of a mixture of anti-CII mAbs followed by i.p. injection of LPS 3 d later (Fig. 4A). Mice with clinical signs of disease at day 6 were randomized and given a single i.p. injection of Fc-μTP-L309C or IVIG, and disease was clinically evaluated up to day 14; untreated mice (PBS only)

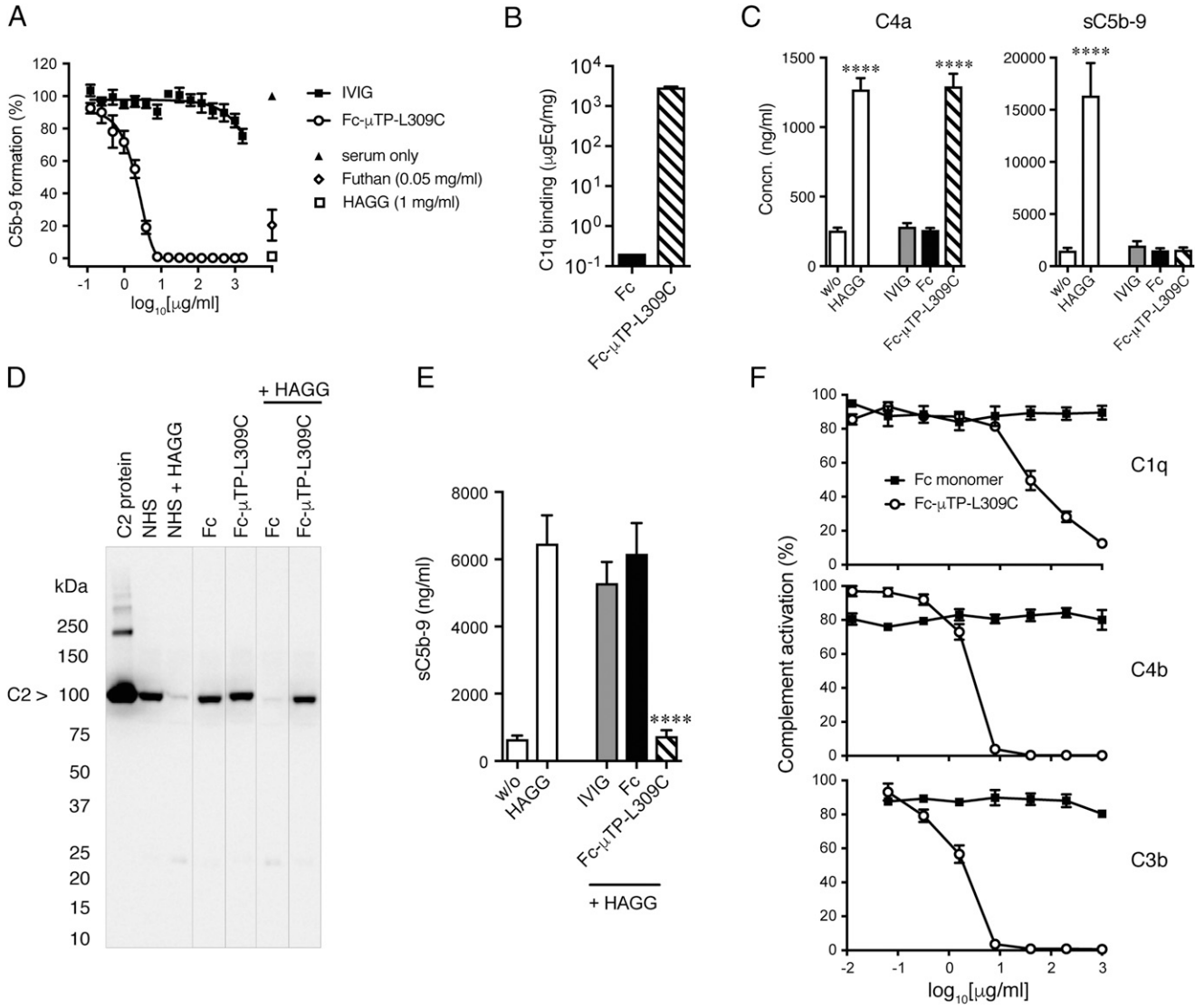

FIGURE 7. Effects of Fc-μTP-L309C on human complement in vitro. (**A**) Inhibition of classical complement pathway by Fc-μTP-L309C. Wieslab ELISA Complement system kit was used. Data show the percentage of C5b-9 formation normalized to NHS values (mean ± SEM, $n = 3$). HAGG and Futhan served as controls. (**B**) Fc and Fc-μTP-L309C binding to C1q, determined by ELISA (mean ± SD, $n = 2$). (**C**) Effect of Fc-μTP-L309C on the generation of C4a (left) and sC5b-9 (right) in human whole blood. HAGG served as a positive control (mean ± SEM, $n = 4$). $^{****}p < 0.0001$, one-way ANOVA with Dunnett test, compared with nonactivated. (**D**) Effect of Fc-μTP-L309C on C2 cleavage in the presence and absence of HAGG, demonstrated by SDS-PAGE and Western blot for C2. The position of C2 is indicated by the arrow; molecular weight markers are shown at left in kiloDaltons. Representative Western blot from three independent experiments. (**E**) Inhibition by Fc-μTP-L309C (1 mg/ml) of sC5b-9 generated in response to HAGG (1 mg/ml) in human whole blood (mean ± SEM, $n = 4$). $^{****}p < 0.0001$, one-way ANOVA with Dunnett test, compared with HAGG. (**F**) Dose-dependent inhibition of C1q, C4b, and C3b deposition on HUVECs by Fc-μTP-L309C, but not Fc monomer (mean ± SEM, $n = 4$).

served as control. Fc-μTP-L309C (200 mg/kg) reduced the clinical signs of disease more rapidly than IVIG (2000 mg/kg), with effects being evident within 24 h and sustained until day 14 (Fig. 4B). With 50 mg/kg a statistically nonsignificant trend to reduced clinical scores was observed (data not shown). Similarly, rapid and persistent effects were achieved via the s.c. route (I.K. Campbell, S. Koernig, and A.W. Zuercher, unpublished observations).

The reduced disease was reflected in the lower numbers of infiltrating ($CD45^+$) leukocytes recovered from knee joints of mice treated with Fc-μTP-L309C at day 8 of disease (Fig. 4C). Histopathology of the arthritic joints confirmed the clinical assessment; reduced inflammatory cell infiltrate, synovitis, and cartilage and bone destruction were evident in the Fc-μTP-L309C–treated mice as early as 48 h after treatment (day 8 in Fig. 4D, 4E).

To further examine the effects of Fc-μTP-L309C on the local inflammatory response, we evaluated cytokine/chemokine levels in joint tissue washes at day 8 using protein arrays. Compared with the PBS control, Fc-μTP-L309C reduced the levels of the proinflammatory cytokines IL-6, LIF, and G-CSF, as well as the chemokines IP-10 (CXCL10), MCP-1 (CCL2), KC (CXCL1), RANTES (CCL5), and MIP-2 (CXCL2) (Supplemental Fig. 1). The multimer did not reduce the levels of IL-9, MIG (CXCL9), or eotaxin (CCL11). In contrast, IVIG had minimal impact on the cytokine/chemokine levels at day 8, with a significant reduction observed only for MIP-2. This could reflect the slower kinetics of the IVIG response (Fig. 4B), which we previously reported in this model (14).

Fc-μTP-L309C reduces complement activation in arthritic mouse joints

To determine whether Fc-μTP-L309C could alleviate disease through an effect on the complement system, we treated arthritic

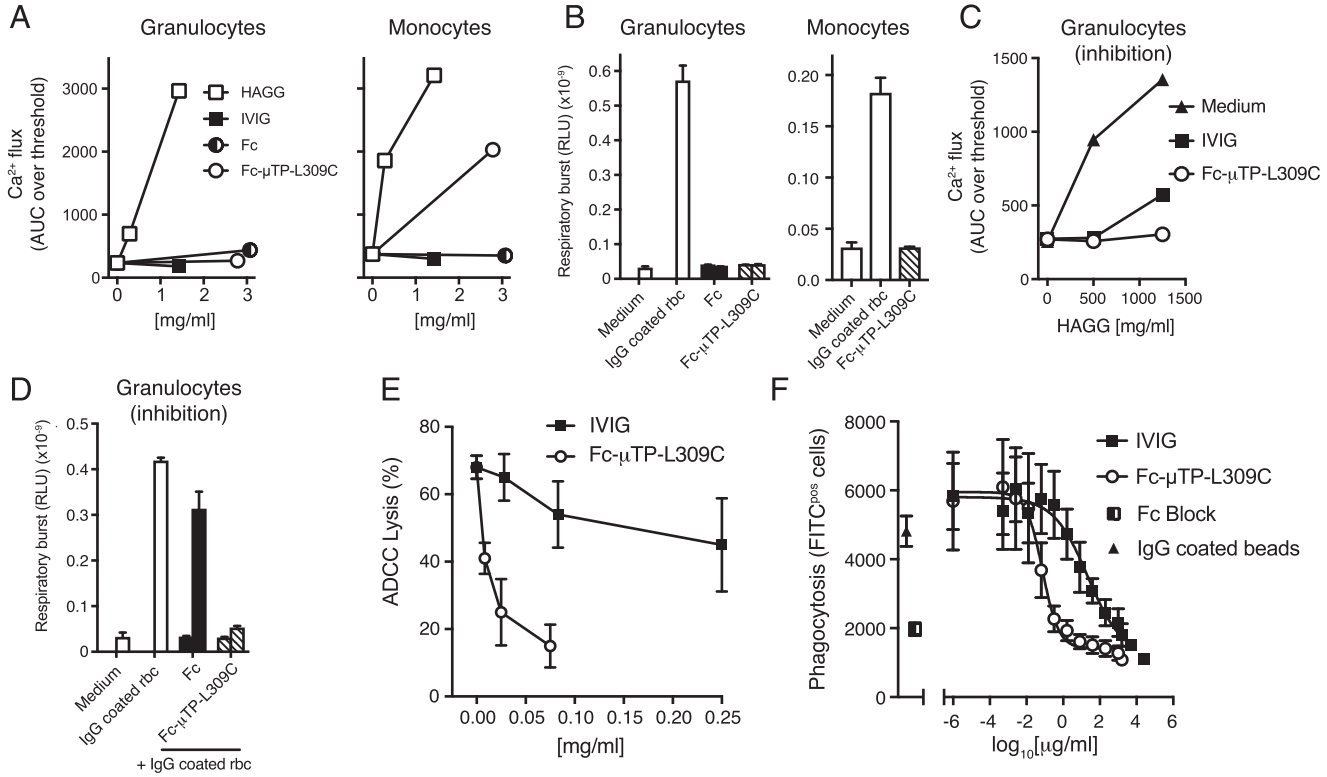

FIGURE 8. Effect of Fc-μTP-L309C on Fc receptor expression and function. (**A**) Induction of calcium flux in human granulocytes ($n = 4$ experiments) and monocytes ($n = 2$ experiments). HAGG served as positive control; one representative experiment is shown. (**B**) Fc-μTP-L309C fails to activate the respiratory burst in human granulocytes ($n = 4$ experiments) and monocytes ($n = 2$ experiments); one representative experiment is shown. (**C**) Calcium flux in human granulocytes induced by HAGG is inhibited by Fc-μTP-L309C; one representative of four experiments is shown. (B and C) Mean ± SD of duplicates are shown. (**D**) Fc-μTP-L309C inhibits the activation of the respiratory burst in response to IgG-coated rabbit RBCs in human granulocytes. (B and D) Left and right columns are 1.5 and 0.4 mg/ml doses, respectively. (**E**) Inhibition of ADCC of anti-D–treated O^+ human RBCs by Fc-μTP-L309C (mean ± SEM, $n = 3$). (**F**) Inhibition of phagocytosis of IgG-coated FITC-labeled latex beads by THP1 cells. Fc Block was used as control (mean ± SEM, $n = 3$).

mice at day 6 with PBS, IVIG, or Fc-μTP-L309C, and C3 and C5a levels were determined in joint washes by ELISA at day 8. Both complement components were elevated in the joint washes of arthritic mice compared with naive mice (Fig. 4F), whereas Fc-μTP-L309C reduced these levels. In contrast, IVIG treatment only slightly reduced C3, and C5a levels were unaffected.

Fc-μTP-L309C provides therapeutic benefit in the chronic inflammatory collagen-induced arthritis model

Having shown the therapeutic benefit of a single injection of Fc-μTP-L309C in the treatment of acute inflammatory arthritis, we next determined its effect in collagen-induced arthritis (CIA), a model of chronic inflammatory autoimmune disease. In CIA, mice generate a continuous supply of anti-CII autoantibodies following immunization with CII, resulting in chronic disease, which enables the evaluation of a prolonged treatment regimen with multiple drug injections. DBA/1 mice were immunized and boosted with chick CII in CFA (27) and treated on the first day of clinical disease with s.c. injection of Fc-μTP-L309C (200 mg/kg), IVIG (2000 mg/kg), or PBS. The mice were monitored for 28 d, and treatment was repeated as outlined in Fig. 5A. As observed in the CAbIA model, Fc-μTP-L309C (at 200 mg/kg) rapidly reduced disease (within 24 h), whereas IVIG (at 2000 mg/kg) was also effective, but the response was relatively delayed (Fig. 5B). Repeated Fc-μTP-L309C injections were necessary to sustain the therapeutic response as disease returned when treatment was ceased for 8 d (see Fig. 5B, days 15–23). Histological evaluation confirmed the clinical findings, with both Fc-μTP-L309C and IVIG significantly reducing disease (inflammatory cell infiltrate and tissue destruction) (Fig. 5C, 5D).

Fc-μTP-L309C provides therapeutic benefit in a murine ITP model

The therapeutic effect of Fc-μTP-L309C was tested in a murine ITP model (Fig. 6). Mice were treated with a single dose of Fc-μTP-L309C (200 mg/kg) when the platelet nadir was attained 2 d after initiating Ab-mediated depletion. Treatment with Fc-μTP-L309C resulted in increased platelet numbers, which were significantly higher at days 3 and 4 ($p < 0.01$ and $p < 0.0001$, respectively, two-way ANOVA with Tukey test) than for mice treated with a 10-fold larger dose of IVIG (2000 mg/kg) (Fig. 6).

Fc-μTP-L309C inhibits complete classical complement pathway activation and is C1q dependent

Because an attenuated complement response was observed in arthritic mice (Fig. 4F), we investigated whether Fc-μTP-L309C interfered with complement activation. Using the Wieslab ELISA Complement system screen kits, we found that Fc-μTP-L309C inhibited the full activation of the CP and LP complement pathways but had no effect on the AP (Fig. 7A, Supplemental Fig. 2A). Furthermore, we have evaluated the effect of Fc-μTP-L309C on the CP without preincubation of rFc multimer with serum. As shown in Supplemental Fig. 3A, Fc-μTP-L309C still prevented C5b-9 formation with similar potency. These findings were confirmed in hemolytic CP and AP complement assays using sheep and rabbit RBCs, respectively (data not shown).

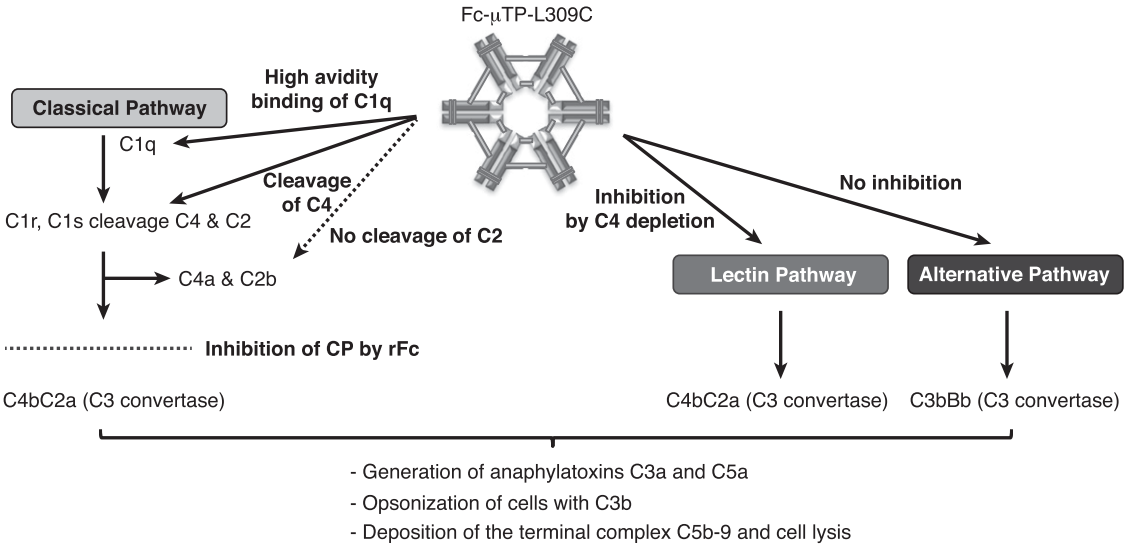

FIGURE 9. Effects of rFc constructs on human complement. Inhibition of the classical complement pathway by Fc-μTP-L309C. High-avidity binding of C1q and subsequent depletion of C4, but no downstream activation of the complement cascade. Consequently, Fc-μTP-L309C inhibits generation of anaphylatoxins C3a and C5a, opsonization by C3b, and deposition of the terminal membrane attack complex C5b-9.

Next, we examined in detail the effect of Fc-μTP-L309C on the CP. We observed incomplete activation of the CP, evidenced by strong binding to C1q (Fig. 7B) and cleavage of C4 (Fig. 7C, Supplemental Fig. 2B), but no generation of sC5b-9 (Fig. 7E) and C5a (Supplemental Fig. 2B). Interestingly, it appeared that activation of the CP stalled at the assembly of the C3 convertase because there was no evidence for cleavage of C2 (Fig. 7D). As the next step, we investigated whether the inhibitory effect of Fc-μTP-L309C on the LP is C1q dependent. As shown in Supplemental Fig. 4A, no cleavage of C4 was observed when Fc-μTP-L309C was incubated in C1q-depleted serum. Furthermore, no inhibition of the LP was observed when Fc-μTP-L309C was incubated in C1q-depleted serum, whereas the inhibitory effect was restored when C1q-depleted serum was reconstituted with purified C1q (Supplemental Fig. 4B). As a control, C1q-depleted serum was tested in the CP and, as expected, the CP was inactive, but activity was restored when reconstituted with purified C1q (Supplemental Fig. 4B). Surprisingly, we observed a reduced activity in C1q-depleted serum reconstituted with purified C1q in the LP. Purified C1q from two different distributors were tested with similar results.

The effect of Fc-μTP-L309C on activation of the CP mediated by HAGG was also investigated (Fig. 7D, 7E). As observed earlier (Fig. 7C), preincubation of human serum or whole blood with Fc-μTP-L309C led to the generation of C4a, which was not further affected by subsequent addition of HAGG (data not shown). However, the Fc-μTP-L309C fully inhibited further downstream activation of the CP, as shown by the inability of HAGG to induce cleavage of C2 (Fig. 7D) or promote the formation of sC5b-9 (Fig. 7E) and C5a (data not shown). Next, we investigated whether Fc-μTP-L309C still inhibited HAGG-induced sC5b-9 formation when given simultaneously and in less diluted whole blood (90% whole blood instead of the 20% whole blood shown in Fig. 7D). As shown in Supplemental Fig. 3B, Fc-μTP-L309C significantly prevented sC5b-9 formation even under these assay conditions.

Fc-μTP-L309C inhibits complement deposition on human endothelial cells in vitro

We investigated whether Fc-μTP-L309C prevented complement deposition on cells in a more physiological system using a complement fragment deposition assay with HUVECs (see *Materials and Methods*). Incubation of opsonized HUVECs with serum containing Fc-μTP-L309C resulted in a dose-dependent inhibition of C1q, C4b, and C3b deposition (Fig. 7F), whereas monomeric Fc or IVIG did not have an effect at the same doses (data not shown for IVIG). As the next step, we investigated whether Fc-μTP-L309C could still prevent complement deposition without preincubation or even postactivation. As shown in Supplemental Fig. 3C, Fc-μTP-L309C still inhibited C3b deposition when given simultaneously or even up to 15 min postactivation.

Fc-μTP-L309C inhibits FcγR-mediated functions in vitro

Next we investigated whether the anti-inflammatory effect of Fc-μTP-L309C, as observed in the arthritis models, might be caused by modulation of FcγR function. Human in vitro systems were used for this purpose. Exposure to Fc-μTP-L309C did not lead to calcium flux or respiratory burst in primary human granulocytes (Fig. 8A, 8B). In contrast, Fc-μTP-L309C induced calcium flux in monocytes (Fig. 8A), but no respiratory burst (Fig. 8B). Importantly, preincubation of granulocytes with Fc-μTP-L309C inhibited subsequent calcium flux induced by HAGG (Fig. 8C) and respiratory burst induced by IgG-coated RBCs (Fig. 8D). In more complex and functional in vitro systems, Fc-μTP-L309C inhibited ADCC (Fig. 8E) and reduced FcγR-mediated phagocytosis (Fig. 8F). Taken together, our data suggest that, in addition to effects on the complement pathways (summarized in Fig. 9), blockade of FcγRs is another possible anti-inflammatory effector mechanism of Fc-μTP-L309C.

Discussion

In this study, we describe the functional characterization of a hexameric IgG1-Fc molecule, termed Fc-μTP-L309C, that was designed to therapeutically block effector pathways in immune complex-mediated diseases. Indeed, Fc-μTP-L309C effectively and rapidly suppressed established acute (Fig. 4B) and chronic arthritis (Fig. 5B), as well as ITP (Fig. 6), in mice. Importantly, these effects were achieved with 10-fold lower doses than IVIG and were reproduced using s.c. administration in the arthritis models. The main mechanisms responsible for these effects are likely to be inhibition of FcγR-mediated effector functions of pathological autoantibodies and inhibition of the CP. Blockade of

FcRn could be an additional mechanism potentially contributing to the therapeutic effects.

The concept of generating IgG1 hexamers by C-terminal fusion with the IgM μ-tailpiece was originally described by Smith et al. (35) using full-length IgG. Hexameric IgG1 Fc molecules were described more recently as a potential carrier for vaccine Ags (36) and subsequently as a therapeutic candidate (21). Initially, in these studies an additional mutation of the Fc sequence at position 310 was proposed (36). This additional mutation appeared to destabilize the hexameric structure (36), and it abolished binding to FcRn (21). Therefore, in their later work the authors focused on a variant with the L309C mutation only (21). This molecule was analyzed structurally, for its binding to Fc receptors and other receptors, as well as for complement activation when bound to solid phase. No analyses of the effect on complement activation under more physiological conditions were performed; likewise, the molecule was not studied in animal models of inflammatory disease (21). More recently, an IgG1/IgG4 hybrid hexameric Fc molecule has also been described (37).

In our experiments, we showed that introducing the L309C mutation stabilized the hexameric structure, demonstrated by the higher proportion of hexameric species in the L309C mutant compared with the WT sequence by SDS-PAGE (Fig. 1B). Interestingly, both SEC-MALS and A4F analyses indicated the presence of ~85% hexamers in both the Fc-μTP and Fc-μTP-L309C, suggesting that a large proportion of the hexamers in Fc-μTP were associated noncovalently (Table I). For this reason, subsequent studies were performed exclusively with the more stable Fc-μTP-L309C molecule.

As expected, hexamerization of IgG-Fc led to a dramatic increase in binding avidity to FcγRs (Fig. 2A). This finding is in line with recent reports on other multimeric Fc molecules such as the Stradomer (17), hexameric Fc (21, 22), and Fc3Y (20). Ortiz et al. (20) established that structures with more than three Fc fragments led to Syk and ERK phosphorylation; furthermore, a trimeric lead molecule (Fc3Y) did not activate but, on the contrary, potently inhibited immune complex-mediated effector cell activation. Indeed, the activation of innate cells through FcγR would not be a desirable property of an Fc multimer in the treatment of autoimmune diseases. Therefore, we investigated in detail the effect of Fc-μTP-L309C on granulocytes and monocytes. In vitro, exposure of monocytes to Fc-μTP-L309C under serum-free conditions led to calcium-flux, an effect that was not seen in granulocytes (Fig. 8A). Importantly, despite this apparent activation of monocytes, no signs of unwanted downstream cellular effector functions were detected, including the absence of respiratory burst in neutrophils and monocytes (Fig. 8B) and platelet activation. Importantly, similar to the Stradomer and Fc3Y, Fc-μTP-L309C potently inhibited disease-relevant Fc-mediated effector functions, such as ADCC and phagocytosis and the CP (see later).

The FcRn has an important role in protecting IgG from degradation and therefore contributing to the extended $t_{1/2}$ of serum IgG, including pathogenic Abs. Enhanced degradation of autoantibodies and alleviation of autoimmune symptoms have been demonstrated after treatment of animals with molecules competing for binding of IgG to FcRn (38), and such molecules are currently in clinical development (39). Fc-μTP-L309C bound to FcRn with high avidity (Fig. 3A), and so it may block recycling of IgG through FcRn, thereby increasing autoantibody degradation. Overall, the importance of FcRn blockade as an effector mechanism of Fc-μTP-L309C will need to be further investigated, and studies are currently under way to examine the ability of Fc-μTP-L309C to use FcRn-mediated recycling pathways.

The potential impact of the short vascular $t_{1/2}$ of Fc-μTP-L309C will need to be studied in more detail. Fc-μTP-L309C showed profound and sustained efficacy in the CAbIA (Fig. 4B) and ITP mouse models (Fig. 6). The short $t_{1/2}$ of Fc-μTP-L309C should not have a great impact in these models because they both rely on passively administered autoantibodies against CII and platelets, respectively, for disease induction and, therefore, have a short therapeutic window for drug testing. For this reason, we further tested Fc-μTP-L309C in the chronic CIA model, in which mice were immunized with CII to produce anti-CII autoantibodies. In this model, the effect of Fc-μTP-L309C seemed less sustained (Fig. 5B). The reduced duration of therapeutic efficacy might be attributed to the short $t_{1/2}$ of Fc-μTP-L309C or the development of an immune response against the human protein upon repeat dosing. Efficacy studies are currently ongoing using a mouse surrogate rFc multimer to minimize the potential effect of anti-drug Abs. Ultimately, immunogenicity and pharmacokinetics studies in nonhuman primates and humans will be required to determine the longevity of the therapeutic effect of Fc-μTP-L309C.

The protective effects of Fc-μTP-L309C appeared to be mediated by a "collaboration" of various mechanisms of action. First, in the CAbIA model, Fc-μTP-L309C inhibited activation of complement, evidenced by decreased levels of C3 and C5a at the inflammatory site (the joint) (Fig. 4F). Because the ELISA used does not discriminate between C3, C3b/c, or C3a, Fc-μTP-L309C might have prevented leakage of uncleaved C3 from the periphery into the joints or decreased generation of C3a by reduced cleavage of local C3 present. In vitro analyses confirmed inhibition of the activation of the CP and LP (Fig. 7A, Supplemental Fig. 2A). Further in-depth in vitro analyses on the interference of Fc-μTP-L309C with complement activation showed partial activation of the CP up to cleavage of C4 (Fig. 7C), but a failure to cleave C2 (Fig. 7D). Thus, no inflammatory downstream products such as C5a (Supplemental Fig. 2B), sC5b-9 (Fig. 7E), or cell-bound C3b (Supplemental Fig. 3C) or C5b-9 (Fig. 7A) were generated (see Fig. 9 for overview). This functional feature is surprising and appears to be unique to Fc-μTP-L309C compared with similar molecules. For example, Ortiz et al. (20) reported no significant impact of the trimeric Fc molecule on complement activation. Studies with Hexa-Fc (21) bound to a solid phase indicated full complement activation; therefore, the inhibitory activity of Fc-μTP-L309C in solution was unexpected. A similar complement inhibitory activity was most recently reported by Zhou et al. (40), demonstrating that GL-2045 bound C1q, leading to generation of C4a, but limited levels of C3a and no C5a. In a second publication, the same group reported novel versions of the Stradomer with reduced binding to FcγRs but intact capability of inhibiting full complement activation (41). Second, FcγR-mediated effector functions relevant to pathological autoantibodies for mediating disease were effectively inhibited by Fc-μTP-L309C, including inhibition of respiratory burst (Fig. 8D), phagocytosis (Fig. 8F), and ADCC (Fig. 8E). These findings are in line with previous data obtained with similar molecules (17, 20). Third, as mentioned earlier, blockade of FcRn may be an additional protective mechanism.

In summary, we describe a unique rFc hexamer with therapeutic efficacy in multiple models of immune complex–mediated autoimmunity when administered at 10-fold lower doses than IVIG. The multimer mimics IVIG Fc-mediated immunomodulatory effects, in particular blockade of FcγR and inhibition of the CP, and may block Ab recycling through FcRn. Fc-μTP-L309C may be a promising candidate as an alternative to IVIG for the treatment of autoimmune disorders and diseases.

Acknowledgments

We thank the following CSL colleagues for experimental support and for critical inputs: Lisa Hetemann, Alexei Navdaev, Sandra Wymann, Thomas Iff, Sara Täschler, Sara Buser, Annette Gaida, Marlies Illi, Georgina

Sansome, Mike Wilson, Cathy Owczarek, Matt Hardy, Soo San Wan, Jessica Petracca, Esin Donaldson, Therese Lynch, Steve Dower, Anne Verhagen, Helen Cao, Matthias Pelzing, Sylvia Miescher, Beate Peter, and Andrew Nash. We also thank Carlos Bosques (Momenta Pharmaceuticals) for critical input.

Disclosures

All authors except B.J.B.L. and D.R.B. are employees of CSL Ltd./CSL Behring AG. The other authors have no financial conflicts of interest.

References

1. Christian, C. L. 1969. Immune-complex disease. *N. Engl. J. Med.* 280: 878–884.
2. Theofilopoulos, A. N., and F. J. Dixon. 1980. Immune complexes in human diseases: a review. *Am. J. Pathol.* 100: 529–594.
3. Gelfand, E. W. 2012. Intravenous immune globulin in autoimmune and inflammatory diseases. *N. Engl. J. Med.* 367: 2015–2025.
4. Katz-Agranov, N., S. Khattri, and G. Zandman-Goddard. 2015. The role of intravenous immunoglobulins in the treatment of rheumatoid arthritis. *Autoimmun. Rev.* 14: 651–658.
5. Ballow, M. 2011. The IgG molecule as a biological immune response modifier: mechanisms of action of intravenous immune serum globulin in autoimmune and inflammatory disorders. *J. Allergy Clin. Immunol.* 127: 315–323; quiz 324–315. 10.1016/j.jaci.2010.10.030
6. Schwab, I., and F. Nimmerjahn. 2013. Intravenous immunoglobulin therapy: how does IgG modulate the immune system? *Nat. Rev. Immunol.* 13: 176–189.
7. Malik, U., L. Oleksowicz, N. Latov, and L. J. Cardo. 1996. Intravenous gammaglobulin inhibits binding of anti-GM1 to its target antigen. *Ann. Neurol.* 39: 136–139.
8. Rossi, F., and M. D. Kazatchkine. 1989. Antiidiotypes against autoantibodies in pooled normal human polyspecific Ig. *J. Immunol.* 143: 4104–4109.
9. Abe, Y., A. Horiuchi, M. Miyake, and S. Kimura. 1994. Anti-cytokine nature of natural human immunoglobulin: one possible mechanism of the clinical effect of intravenous immunoglobulin therapy. *Immunol. Rev.* 139: 5–19.
10. Fehr, J., V. Hofmann, and U. Kappeler. 1982. Transient reversal of thrombocytopenia in idiopathic thrombocytopenic purpura by high-dose intravenous gamma globulin. *N. Engl. J. Med.* 306: 1254–1258.
11. Hansen, R. J., and J. P. Balthasar. 2002. Intravenous immunoglobulin mediates an increase in anti-platelet antibody clearance via the FcRn receptor. *Thromb. Haemost.* 88: 898–899.
12. Basta, M., L. F. Fries, and M. M. Frank. 1991. High doses of intravenous Ig inhibit in vitro uptake of C4 fragments onto sensitized erythrocytes. *Blood* 77: 376–380.
13. Samuelsson, A., T. L. Towers, and J. V. Ravetch. 2001. Anti-inflammatory activity of IVIG mediated through the inhibitory Fc receptor. *Science* 291: 484–486.
14. Campbell, I. K., S. Miescher, D. R. Branch, P. J. Mott, A. H. Lazarus, D. Han, E. Maraskovsky, A. W. Zuercher, A. Neschadim, D. Leontyev, et al. 2014. Therapeutic effect of IVIG on inflammatory arthritis in mice is dependent on the Fc portion and independent of sialylation or basophils. *J. Immunol.* 192: 5031–5038.
15. Debré, M., M. C. Bonnet, W. H. Fridman, E. Carosella, N. Philippe, P. Reinert, E. Vilmer, C. Kaplan, J. L. Teillaud, and C. Griscelli. 1993. Infusion of Fc gamma fragments for treatment of children with acute immune thrombocytopenic purpura. *Lancet* 342: 945–949.
16. Zuercher, A. W., R. Spirig, A. Baz Morelli, and F. Käsermann. 2016. IVIG in autoimmune disease - Potential next generation biologics. *Autoimmun. Rev.* 15: 781–785.
17. Jain, A., H. S. Olsen, R. Vyzasatya, E. Burch, Y. Sakoda, E. Y. Mérigeon, L. Cai, C. Lu, M. Tan, K. Tamada, et al. 2012. Fully recombinant IgG2a Fc multimers (stradomers) effectively treat collagen-induced arthritis and prevent idiopathic thrombocytopenic purpura in mice. *Arthritis Res. Ther.* 14: R192.
18. Niknami, M., M. X. Wang, T. Nguyen, and J. D. Pollard. 2013. Beneficial effect of a multimerized immunoglobulin Fc in an animal model of inflammatory neuropathy (experimental autoimmune neuritis). *J. Peripher. Nerv. Syst.* 18: 141–152.
19. Thiruppathi, M., J. R. Sheng, L. Li, B. S. Prabhakar, and M. N. Meriggioli. 2014. Recombinant IgG2a Fc (M045) multimers effectively suppress experimental autoimmune myasthenia gravis. *J. Autoimmun.* 52: 64–73.
20. Ortiz, D. F., J. C. Lansing, L. Rutitzky, E. Kurtagic, T. Prod'homme, A. Choudhury, N. Washburn, N. Bhatnagar, C. Beneduce, K. Holte, et al. 2016. Elucidating the interplay between IgG-Fc valency and FcγR activation for the design of immune complex inhibitors. *Sci. Transl. Med.* 8: 365ra158.
21. Czajkowsky, D. M., J. T. Andersen, A. Fuchs, T. J. Wilson, D. Mekhaiel, M. Colonna, J. He, Z. Shao, D. A. Mitchell, G. Wu, et al. 2015. Developing the IVIG biomimetic, hexa-Fc, for drug and vaccine applications. *Sci. Rep.* 5: 9526.
22. Qureshi, O. S., T. F. Rowley, F. Junker, S. J. Peters, S. Crilly, J. Compson, A. Eddleston, H. Björkelund, K. Greenslade, M. Parkinson, et al. 2017. Multivalent Fcγ-receptor engagement by a hexameric Fc-fusion protein triggers Fcγ-receptor internalisation and modulation of Fcγ-receptor functions. *Sci. Rep.* 7: 17049.
23. Diebolder, C. A., F. J. Beurskens, R. N. de Jong, R. I. Koning, K. Strumane, M. A. Lindorfer, M. Voorhorst, D. Ugurlar, S. Rosati, A. J. Heck, et al. 2014. Complement is activated by IgG hexamers assembled at the cell surface. *Science* 343: 1260–1263.
24. Chen, C. G., L. J. Fabri, M. J. Wilson, and C. Panousis. 2014. One-step zero-background IgG reformatting of phage-displayed antibody fragments enabling rapid and high-throughput lead identification. *Nucleic Acids Res.* 42: e26.
25. Schmidt, P. M., M. Abdo, R. E. Butcher, M. Y. Yap, P. D. Scotney, M. L. Ramunno, G. Martin-Roussety, C. Owczarek, M. P. Hardy, C. G. Chen, and L. J. Fabri. 2016. A robust robotic high-throughput antibody purification platform. *J. Chromatogr. A* 1455: 9–19.
26. Spanevello, M. D., S. I. Tajouri, C. Mirciov, N. Kurniawan, M. J. Pearse, L. J. Fabri, C. M. Owczarek, M. P. Hardy, R. A. Bradford, M. L. Ramunno, et al. 2013. Acute delivery of EphA4-Fc improves functional recovery after contusive spinal cord injury in rats. *J. Neurotrauma* 30: 1023–1034.
27. Campbell, I. K., J. A. Hamilton, and I. P. Wicks. 2000. Collagen-induced arthritis in C57BL/6 (H-2b) mice: new insights into an important disease model of rheumatoid arthritis. *Eur. J. Immunol.* 30: 1568–1575.
28. Campbell, I. K., D. Leong, K. M. Edwards, V. Rayzman, M. Ng, G. L. Goldberg, N. J. Wilson, K. Scalzo-Inguanti, C. Mackenzie-Kludas, K. E. Lawlor, et al. 2016. Therapeutic targeting of the G-CSF receptor reduces neutrophil trafficking and joint inflammation in antibody-mediated inflammatory arthritis. *J. Immunol.* 197: 4392–4402.
29. Katsman, Y., A. H. Foo, D. Leontyev, and D. R. Branch. 2010. Improved mouse models for the study of treatment modalities for immune-mediated platelet destruction. *Transfusion* 50: 1285–1294.
30. Leontyev, D., Y. Katsman, X. Z. Ma, S. Miescher, F. Käsermann, and D. R. Branch. 2012. Sialylation-independent mechanism involved in the amelioration of murine immune thrombocytopenia using intravenous gammaglobulin. *Transfusion* 52: 1799–1805.
31. Sørensen, V., V. Sundvold, T. E. Michaelsen, and I. Sandlie. 1999. Polymerization of IgA and IgM: roles of Cys309/Cys414 and the secretory tailpiece. *J. Immunol.* 162: 3448–3455.
32. Kagari, T., D. Tanaka, H. Doi, and T. Shimozato. 2003. Essential role of Fc gamma receptors in anti-type II collagen antibody-induced arthritis. *J. Immunol.* 170: 4318–4324.
33. Nandakumar, K. S., and R. Holmdahl. 2006. Antibody-induced arthritis: disease mechanisms and genes involved at the effector phase of arthritis. *Arthritis Res. Ther.* 8: 223.
34. Banda, N. K., K. Takahashi, A. K. Wood, V. M. Holers, and W. P. Arend. 2007. Pathogenic complement activation in collagen antibody-induced arthritis in mice requires amplification by the alternative pathway. *J. Immunol.* 179: 4101–4109.
35. Smith, R. I., M. J. Coloma, and S. L. Morrison. 1995. Addition of a mu-tailpiece to IgG results in polymeric antibodies with enhanced effector functions including complement-mediated cytolysis by IgG4. *J. Immunol.* 154: 2226–2236.
36. Mekhaiel, D. N., D. M. Czajkowsky, J. T. Andersen, J. Shi, M. El-Faham, M. Doenhoff, R. S. McIntosh, I. Sandlie, J. He, J. Hu, et al. 2011. Polymeric human Fc-fusion proteins with modified effector functions. *Sci. Rep.* 1: 124.
37. Rowley, T., F. Fallah-Arani, and D. Humphreys. 2016. Optimising the effector function balance of Fc-multimers for treatment of auto-antibody mediated disease. In *10th International Congress on Autoimmunity, April 6–19, 2016*. Leipzig, Germany. (Abstr. 658).
38. Patel, D. A., A. Puig-Canto, D. K. Challa, H. Perez Montoyo, R. J. Ober, and E. S. Ward. 2011. Neonatal Fc receptor blockade by Fc engineering ameliorates arthritis in a murine model. *J. Immunol.* 187: 1015–1022.
39. Argenx. A study to evaluate the safety, efficacy, and pharmacokinetics of ARGX-113 in patients with myasthenia gravis who have generalized muscle weakness. Available at: https://clinicaltrials.gov/ct2/show/NCT02965573. Accessed: February 2, 2017.
40. Zhou, H., H. Olsen, E. So, E. Mérigeon, D. Rybin, J. Owens, G. LaRosa, D. S. Block, S. E. Strome, and X. Zhang. 2017. A fully recombinant human IgG1 Fc multimer (GL-2045) inhibits complement-mediated cytotoxicity and induces iC3b. *Blood Adv.* 1: 504–515.
41. Sun, H., H. S. Olsen, E. Y. Mérigeon, E. So, E. Burch, S. Kinsey, J. C. Papadimitriou, C. B. Drachenberg, S. M. Bentzen, D. S. Block, et al. 2017. Recombinant human IgG1 based Fc multimers, with limited FcR binding capacity, can effectively inhibit complement-mediated disease. *J. Autoimmun.* 84: 97–108.